

Donald McCann
Aviation Weather Center
Kansas City MO 64153

1. Introduction

McCann (2001) outlined an ingredients-based clear air turbulence (CAT) forecast technique and presented a "recipe" for combining the ingredients: Gravity waves locally modify the environmental Richardson number which can trigger CAT. In order to apply this technique, characteristics of the gravity wave trigger must be known or estimated, but the paper only hinted at possible gravity wave triggers. This paper describes the development of one trigger mechanism. The verification results show positive skill at both moderate and severe CAT. The results also show an underforecast bias suggesting that this trigger is only one of others.

2. An unbalanced flow/gravity wave trigger

The production of gravity wave enhanced turbulent kinetic energy (TKE_L) is

$$TKE_L = K_m \left(\frac{\partial V}{\partial z} \right)_E^2 \left(1 + Ri_E^{1/2} \hat{a} \sin \phi \right)^2 \quad (1)$$

where K_m is the momentum eddy diffusivity or eddy viscosity, $(\partial V / \partial z)_E$ is the environmental wind shear, Ri_E is the environmental Richardson number, and ϕ is gravity wave phase angle, which locates where in the gravity wave TKE_L is being computed. The non-dimensional wave amplitude (\hat{a}) is

$$\hat{a} = \frac{aN}{|V - c|} \quad (2)$$

where a is the gravity wave amplitude, N is stability (Brunt-Väisälä frequency), V is the wind velocity, and c is the gravity wave phase velocity. The denominator is the Doppler-adjusted wind velocity. The non-dimensional amplitude will be high when any of three variables are sufficiently favorable, 1) high gravity wave amplitude, 2) high stability, and 3) low difference between the wind and wave velocities. The TKE_L is maximized in the portion of the gravity wave where $\phi = \pi/2$ ($\sin \phi = 1$). Since forecasts are for scales much larger than the gravity wave/turbulence scales, useful CAT forecasts need only be for the maximum TKE.

The maximum TKE_L from (1) is only valid for \hat{a} values large enough to reduce Ri_E to a local $Ri_L < 0.25$. If $\hat{a} > 2$, then Ri_L is always less than 0.25. For $\hat{a} < 2$ Ri_E must be less than the curve shown in Figure 1. Below the curve are Ri_E / \hat{a} combinations that are turbulent.

The (\hat{a}, Ri_E) factor in (1) magnifies the environmental wind shear TKE production. McCann (2001) showed that in one case the TKE_L was estimated to be nearly 10 times the TKE production from the environmental wind shear.

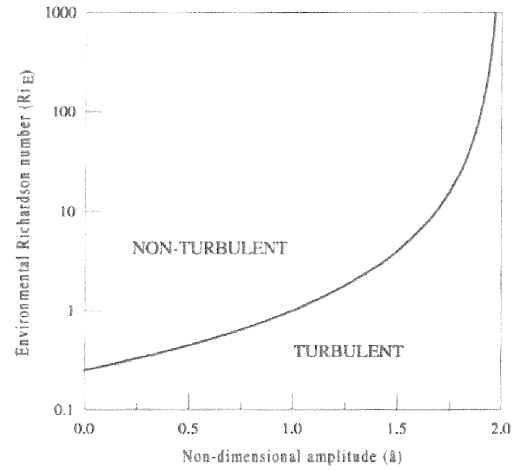


Figure 1. Curve of the bounding value of the environmental Richardson number as a function of the non-dimensional amplitude (\hat{a}). When (\hat{a}, Ri_E) falls in the TURBULENT region, a gravity wave will locally increase the wind shear sufficiently to reduce the local Richardson number to 0.25.

Applying (1) requires knowledge of the non-dimensional wave amplitudes (\hat{a}) which can be computed from (2). However, the actual wave amplitude and phase velocity of a given gravity wave needed to compute \hat{a} are largely unknown. However, one can empirically estimate \hat{a} from the divergence tendency equation.

The Lagrangian time derivative of the continuity equation is

$$\frac{d}{dt} \frac{\partial \omega}{\partial p} = \frac{d}{dt} (-\nabla_H \cdot V) \quad (3)$$

where ω is the vertical velocity in pressure coordinates, p is pressure, and V is the horizontal wind. The left side implies a change in the vertical profile of vertical velocity profile which implies a vertical acceleration. A vertical acceleration must be caused by a vertical force which, with positive stability, causes a gravity wave. Thus the total time derivative of divergence may be used as a proxy for the occurrence of gravity waves.

One can compute the total divergence tendency knowing the divergence at two different times. However, the divergence tendency may be computed from variables at a single time. Taking the divergence of both sides of the equation of motion and after considerable algebra (Haltiner and Williams 1980) the total divergence equation becomes:

$$\begin{aligned} \frac{\partial D}{\partial t} + V \cdot \nabla D + \omega \frac{\partial D}{\partial p} = & -D^2 - \frac{\partial V}{\partial p} \cdot \nabla \omega \\ & \quad \quad \quad A \quad \quad \quad B \\ & + 2J(u, v) - \beta u + f\xi - \nabla^2 \Phi + \nabla \cdot F \\ & \quad \quad \quad C \quad \quad \quad D \quad \quad \quad E \quad \quad \quad F \quad \quad \quad G \end{aligned} \quad (4)$$

where D is the divergence, V is the horizontal wind velocity, u , v , and ω are the three components of total wind velocity, J is the Jacobian operator, f is the Coriolis parameter, β is $\partial f / \partial y$, ξ is the relative vorticity, Φ is the geopotential and F is the frictional force. The left hand side are the three Eulerian components of the Lagrangian time derivative of divergence. On the right side, term A is the effect divergence has on its tendency, term B is the vertical wind shear/horizontal gradient of vertical motion interaction, term C accounts for the horizontal wind shear, and term D is the effect due to the convergence of longitude at the poles. Terms E and F can be summed into an ageostrophic vorticity effect. Term G contains the subgrid processes that change divergence including the turbulence itself. Unfortunately, it cannot be evaluated like the other terms. All lettered terms do not include their mathematical sign. Term D is two orders of magnitude smaller than the other terms and can safely be ignored. All other terms can be significant contributors to divergence tendency.

Terms A , B , and C are called inertial terms because they arise from the acceleration term in the equation of motion. Terms E and F are called forcing terms because they arise from the force terms in the equation of motion.

With the hypothesis that the total divergence tendency causes gravity waves in a stable environment, it is further hypothesized that the magnitude of total divergence tendency is proportional to and may be used to estimate the non-dimensional gravity wave amplitude in (1) to estimate enhanced TKE production.

Terms from (4) were diagnosed from one-hour RUC2 model forecasts to test the hypothesis. First, for a few known strong turbulence outbreak cases, an analysis of each term was displayed along with the associated pilot reports. Term C showed the best positive visual correlation with the reports and the positive sum of terms E and F next best. Interestingly, the results for terms A , B , and C , the inertial terms, showed the best visual correlation when the terms were negative. Term G was calculated as a residual from the time difference of divergence fields but did not show any positive visual correlation.

This initial study suggested a gravity wave indicator (GW) as the negative sum of inertial terms and the positive sum of forcing terms:

$$GW = -(A + B + C) + E + F \quad (5)$$

3. Combining the ingredients

In order to solve (1), the eddy viscosity must be known. McCann (1999) derived a simple K_m in the boundary layer. Implied in the derivation is a constant air density. Aloft, K_m is smaller with height, so a simple adjustment is to multiply the boundary layer K_m by the density, ρ . Thus,

$$K_m = 33.75 \rho(p) \quad (6)$$

A daily set of one hour 15Z RUC2 model forecasts/pilot reports above flight level 15000 feet from February-March, 2002, was examined to find a proportional relationship between GW and $\hat{\alpha}$. The TKE production from (1) was compared with turbulence intensity with a range of proportionality constants. The "best" constant was the one that showed the highest skill at a TKE production threshold of $.035 \text{ j sec}^{-1}$ for severe turbulence, the same threshold in the boundary layer (McCann 1999):

$$\hat{a} = \frac{GW}{c} \quad (7)$$

where $c = 1.2 \times 10^{-8} \text{ sec}^{-2}$. For both physical and computational reasons, \hat{a} was limited to 2.5.

ULTURB is the algorithm that combines the ingredients for upper level turbulence forecasting. Table 1 outlines ULTURB's steps.

Table 1. The ULTURB process

1. Compute \hat{a} and R_i .
2. Determine the (\hat{a}, R_i) combination.
3. If above Fig. 1 curve, $TKE = 0$
4. If below Fig. 1 curve, $TKE = \text{Eq. (1)}$

4. Verification

ULTURB was verified for its skill on an independent database of 7584 turbulence pilot reports, flight level > 15000 feet, and daily one hour 15Z RUC2 forecasts from November, 2002 through March, 2003. Each verified report was within one hour of 16Z. Table 2 compares the results with other standard turbulence forecast aids.

Although significantly different from any other turbulence aid, ULTURB's overall skill score is only slightly better than traditional forecast techniques. There is a difference in character as evidenced by the other statistics. ULTURB forecasts turbulence more conservatively than the other aids. The bias indicates that this leads to significant underforecasting indicating that the total divergence tendency terms are not the only turbulence trigger mechanism. Additional research will hopefully discover other triggers.

As a sidebar, other combinations of divergence tendency terms were verified with this database, but none tested as well as ULTURB.

Table 2. Verification results for four turbulence aids. PODY is probability of detection of reports at least the intensity. PODN is the probability of detection of reports below the intensity. HSS is the Heidke Skill Score.

ULTURB	Threshold sec^{-1}	PODY	PODN	HSS	Bias
LGT	.0001	.231	.953	.154	.262
MOD	.001	.327	.911	.275	.567
SEV	.035	.231	.983	.231	.854
<u>Ellrod Index sec^{-2}</u>					
LGT	5e-7	.410	.806	.193	.537
MOD	7.5e-7	.367	.849	.233	.771
SEV	2.5e-6	.241	.971	.182	1.332
<u>Wind shear² sec^{-2}</u>					
LGT	5e-5	.514	.646	.149	.746
MOD	1e-4	.380	.781	.163	.966
SEV	5e-4	.156	.981	.148	.844
<u>Richardson Number</u>					
LGT	5	.658	.601	.259	.919
MOD	2	.471	.778	.246	1.061
SEV	.5	.266	.976	.226	1.151

Note: Ellrod and Knapp (1992) define the Ellrod Index.

5. A case study

The largest outbreak of severe turbulence in the final verification set occurred on 13 November 2002. Figures 2-5 illustrate the value of each term in the total divergence tendency trigger diagnostic. Each of the terms in (5) computed in the 375:400 mb layer (near FL250) are displayed in the region of interest. Figure 6 shows the resulting ULTURB TKE production and the pilot reports received between 15 UTC and 17 UTC and between FL220 and FL280. Severe turbulence occurred as low as FL160 during this period.

The 2×2 contingency table (Table 3) shows that ULTURB had considerable skill diagnosing the significant turbulence on this day.

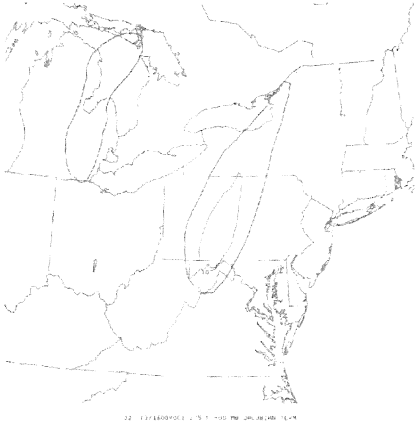


Figure 2. Jacobian term (C) in (5) diagnostic from the one-hour RUC2 model forecast at 15 UTC 13 Nov 2002. Units are 10^9 sec^{-2} . Only values less than -5 are contoured.

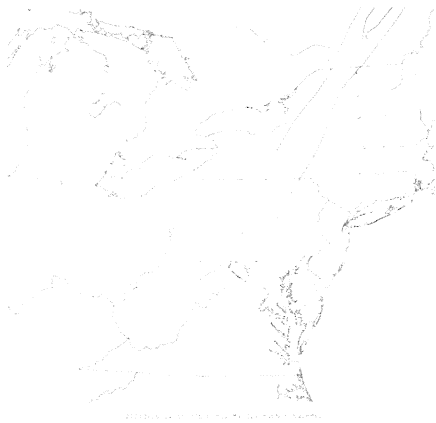


Figure 3. Same as Figure 2 except for divergence squared term (A) in (5). Only values > 5 are contoured.

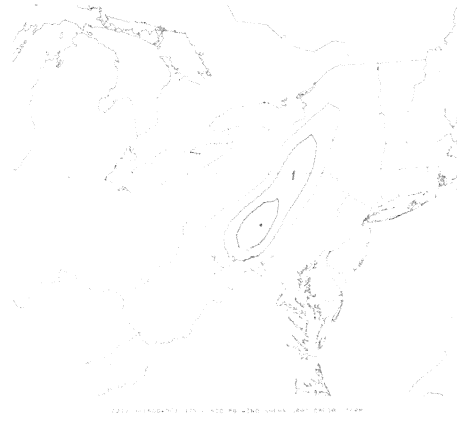


Figure 4. Same as Figure 3 except for the wind shear/gradient omega term (B) in (5).

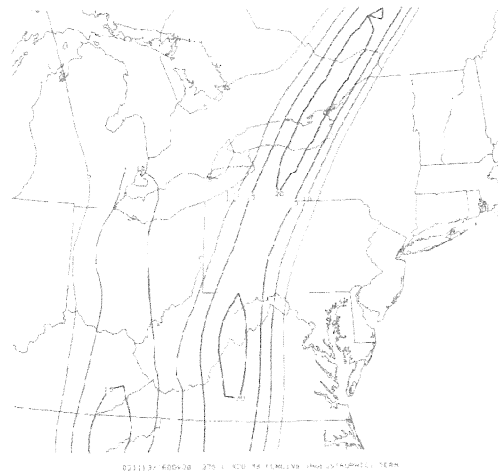


Figure 5. Same as Figure 3 except for the forcing (ageostrophic) term (E+F) in (5).

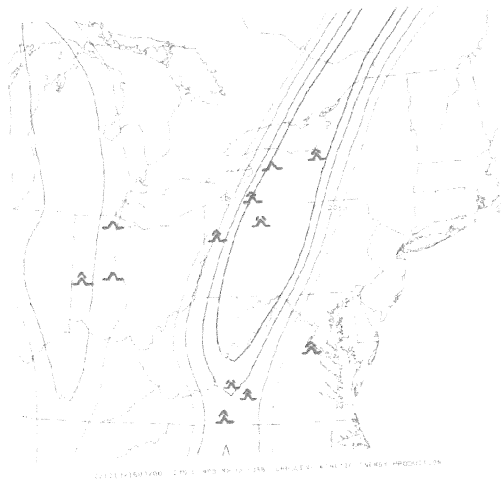


Figure 6. Contoured display of ULTURB TKE production computed from the one-hour 15 UTC 13 Nov 2002 RUC2 model forecast. Units are 10^3 j sec^{-1} . Pilot reports from 15 UTC to 17 UTC are plotted with conventional symbols.

Table 3. 2×2 contingency table of the one-hour from 15 UTC 13 Nov 2002 RUC2 forecast ULTURB TKE production $> .035 \text{ j sec}^{-1}$ and the pilot reports of moderate-severe or greater turbulence over the United States plus or minus one hour from 16 UTC.

Forecast	Observed	
	yes	no
yes	36	29
no	10	84

6. Conclusion

ULTURB implements the McCann (2001) ingredients-based upper level turbulence forecast technique. The results suggest that only a negative sum of the inertial terms and a positive sum of the forcing terms have diagnostic value. These results are combined into a single diagnostic algorithm (relevant total divergence tendency terms \rightarrow gravity wave occurrence/amplitude/phase velocity \rightarrow TKE production) to provide CAT forecast guidance.

References

Ellrod, G.P. and D.I. Knapp, 1992: An objective clear-air turbulence forecasting technique: Verification and operational use. *Wea. Forecasting*, **7**, 150-165.

Haltiner, G.J. and R.T. Williams, 1980: *Numerical Prediction and Dynamic Meteorology*, John Wiley and Sons, New York NY, 477 pp.

McCann, D.W., 1999: A simple turbulent kinetic energy equation and aircraft boundary layer turbulence. *Natl. Wea. Digest*, **23** (1,2), 13-19.

_____, 2001: Gravity waves, unbalanced flow, and aircraft clear air turbulence. *Natl. Wea. Digest*, **25** (1,2), 3-14.